Characterizing mmWave radio propagation at 60GHz in a conference room scenario

Aleksei Ponomarenko-Timofeev[1][0000−0001−5734−2253],
Vasilii Semkin[1][0000−0003−2058−0754],
Pavel Masek[3][0000−0003−2976−6547], and
Olga Galinina[1][0000−0002−5386−1061]

[1] Tampere University of Technology, Tampere, Finland
[2] Peoples Friendship University of Russia (RUDN University), Russian Federation
[3] Brno University of Technology, Brno, Czech Republic

Contact author's e-mail: aleksei.ponomarenko-timofeev@tut.fi

Abstract. In this paper, we provide a shooting and bouncing ray (SBR) based simulation study of mmWave radio propagation at 60 GHz in a typical conference room. The room geometry, material types, and other simulation settings are verified against the results of the measurement campaign at 83 GHz in [15]. Here, we extend the evaluation scenario by randomly scattering several human-sized blockers as well as study the effects of human body blockage models. We demonstrate that multiple knife-edge diffraction (KED) models are capable of providing meaningful results while keeping the simulation duration relatively short. Moreover, we address another important scenario, where transmitters and receivers are located at the same heights and are moving according to a predefined trajectory that corresponds, for example, to device-to-device interactions or inter-user interference.

Keywords: mmWave · 60GHz · radio propagation · indoor propagation · conference room.

1 Introduction

The growing popularity of data-intensive sophisticated mobile and wearable devices is likely to cause a new surge of wireless data demand in the near future. However, the frequency spectrum below 6 GHz, highly populated today, will not be capable of accommodating the increased data traffic from various rate-hungry hi-tech devices that might flood the wireless market quite soon. To facilitate this growing demand the research community draws its attention to novel millimeter-wave systems, which due to the evolution of integrated circuits, progressively become available for multiple consumer and industrial use-cases in both indoor and outdoor scenarios [17].

In the light of this, in July 2016, the Federal Communications Commission (FCC) introduced a new guideline for the licensed operation of millimeter-wave (mmWave) bands (centered at 28, 37, and 39 GHz[1]) as well as extended the regulations for the unlicensed 60 GHz frequency band (from 57 - 63 GHz to 71 GHz).

[1] Report and Order and Further Notice of Proposed Rule-making, document FCC-16-89, Federal Communication Commission, Jul. 2016.

In the aggregate, the nearly 11 GHz of frequency spectrum has been released, which opens up fundamentally new prospects for future wireless systems.

1.1 Motivation

In contrast to legacy frequencies below 6 GHz, the mmWave band offers channels with contiguous bandwidth orders of wider magnitude, hence accelerating the communications to multi-Gbps rates per link [23]. However, despite the high potential of mmWave communications, they come with many fundamental challenges. For example, while in an outdoor mesh network at 60 GHz high transmission directivity mitigates the interference between nonadjacent links [22], in indoor scenarios, due to the limited space, the assumption of "pseudowired" links may not be sufficiently accurate, and the signal propagation becomes less favorable.

To evaluate the system performance realistically, it is imperative to understand the behavior of a 60 GHz channel impulse response and to develop adequate channel models, which may be derived using the data obtained in the course of measurement campaigns or by running shooting and bouncing ray (SBR) simulation tools (see, for example, [16, 21]). As human blockage is one of the most significant aspects of indoor mmWave communications, it attracts considerable attention from the research community [7, 19, 10], resulting in a wide variety of proposed models, including cylinders, knife-edge models, and cuboids [5, 14, 11].

In particular, most of the research efforts focus on the following three typical models for a human blocker: (i) circular cylinder – perfectly conducting cylinder (PEC) [18], dielectric cylinder [2]; dielectric-coated perfectly conducting cylinder [25]; (ii) dielectric elliptic cylinder [24]; (iii) and multiple knife-edge diffraction (MKED) model [10].

In this work, we focus on studying indoor signal propagation at 60 GHz in a conference room and in the presence of human blockers, which are simplified to MKED and elliptic cylinder models. After calibrating with openly available measurement data for 83 GHz, we perform a comparison of MKED and elliptic cylinder models in terms of performance and propagation paths. After that, we provide the results of SBR simulation for the said two types of human blocker models at 60 GHz.

1.2 Main Contributions

Although the properties of the mmWave channel have received considerable attention in the past, the assumptions under which the majority of channel models have been developed, however, limit their use to standard "a device to an access point" links and cannot be directly applied to, for example, typical body-centric applications.

To fill this gap, we reconstruct an indoor scenario where multiple users carry wearable or hand-held mobile devices, potentially forming device-to-device (D2D) links [26, 12] or causing interference [26] from the neighboring devices. The main contributions of this paper are as follows:

– Analysis of the effects of the human body blockage at 60 GHz for D2D links in a conference/lecture room (see Fig.1).
– Detailed discussion and comparison of different human body models, i.e., MKED and elliptic cylinder models within the studied scenario.

The paper is organized as follows. Section II briefly introduces our scenario of interest, as well as the process of calibration for 83 GHz. In Section III, we present simulation results for 60 GHz frequency band in the presence of human blockers and compare the effect of different human body models. Section IV refers to a D2D use-case and analyzes the simulation results for the case of the transmitter and receiver, moving along selected trajectories located at the same heights. Finally, Section V outlines the main conclusions of our study.

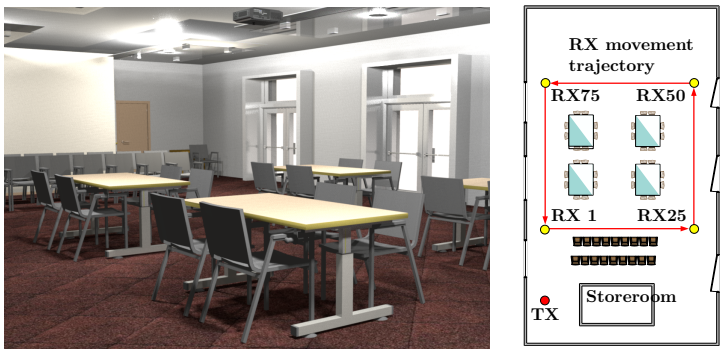

(a) 3D model (b) Floor plan

Fig. 1: A 3D model of the conference room and a schematic top view of the room, with the receiver positions.

2 Our Scenario and Calibration with Measurement Data

In this work, we study radio channel propagation properties using the SBR method for a conference room 3D model (Fig. 1). To perform the simulations, we employ a commercial tool named Wireless Insite (Remcom), which is specifically developed for modeling signal propagation in various environments.

First, to calibrate our simulation tool settings and verify the correctness of our modeling approach, we study the scenario mentioned above at 83 GHz and compare the obtained results with the measurement data from [15]. In particular, we replicate the geometry of the conference room according to the available plan and specify the material properties so that our analysis corresponds to the measured results. We specify several materials, dominant in this scenario, such as wood, glass, and gypsum drywall. The electrical properties of these materials may be found in Table 1, while other simulation parameters are given in Table 2. For the better tractability of the results, omnidirectional antennas are assumed at the transmitter and the receiver side with 0 dBi gain, while the transmit power is set to 0 dBm.

Table 1: Material parameters

Material	**Conductivity [S/m]**	**Relative permittivity**	**Thickness [mm]**
Wood	0.000	5.00	30.0
Glass	0.567	6.27	3.0
Gypsum drywall	0.001	2.80	12.7

Table 2: Core simulation settings.

Parameter	**Transmitter**	**Receiver**
Antenna type	Isotropic	Isotropic
Gain (G)	0 dBi	0 dBi
Polarization	Vertical	Vertical
Input power	0 dBm	-
Transmission line loss	0 dB	-
Noise Figure	-	3 dB
Antenna heights	2.5 m	1.6 m
Location number	1	100

To verify the configuration of our scenario, we compare the simulation and measurement results as follows. Fig. 2 shows the modeled angular delay profile for the line-of-sight (LOS) and multipath components (MPC) in comparison to the measured data [15]. The results for the LOS component are almost identical, while the first order MPCs obtained by ray-based modeling are reasonably close to the measurement data. Although the latter demonstrates a slight visual difference, this may be explained by the fact that the model used in the simulation does not include small details present in the real room.

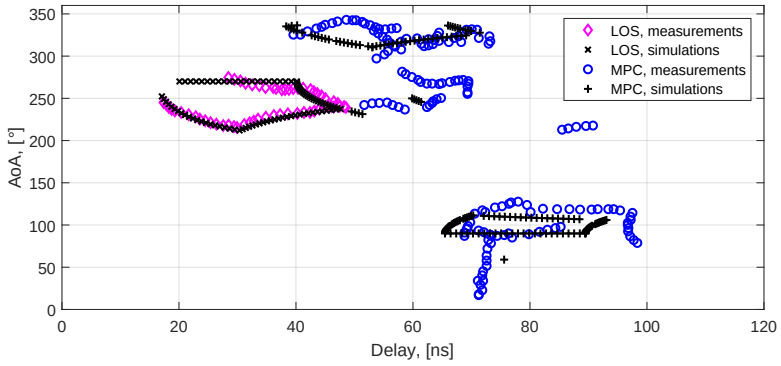

Fig. 2: Calibrating the SBR software. Comparison between the measurements from [15] and simulation results for LOS and MPC at 83 GHz.

3 Simulation results at 60 GHz

3.1 Human body blockage models

Wireless links at 60 GHz may provide up to 1.5 Gbit/s (assuming single carrier modulation and coding scheme MCS-6) [27], which is more than sufficient for HD video streaming. However, higher signal attenuation caused by human body presence causes certain limitations in terms of using the LOS link as a primary option at 60 GHz. Therefore understanding of multipath propagation characteristics is crucial for the further improvement of the network performance. The

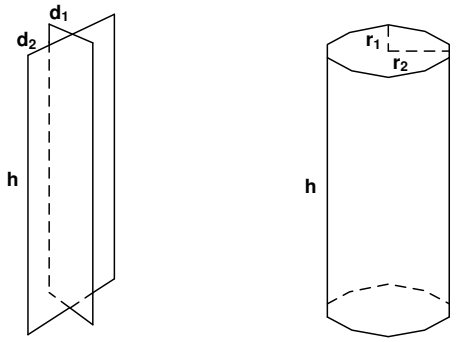

(a) MKED model (b) Cylindrical model

Fig. 3: MKED and elliptic cylinder human body models used in the SBR simulations, where $h = 1.8$ m, $d_1 = 2r_1 = 0.28$ m, $d_2 = 2r_2 = 0.47$ m.

Table 3: Human body model parameters used in the SBR simulations.

Material	**Conductivity [S/m]**	**Relative permittivity**	**Thickness [mm]**
Skin	36.40	7.98	1.26
Muscle	52.83	12.86	5.00

human blockage, as is well known, becomes a critical issue when it comes to the 60 GHz frequency range since mmWave signals are severely attenuated by the human body [3]. Therefore, analysis of human blockage effects in scenarios, which potentially may involve large numbers of human participants, opens one of the most important directions of mmWave research. In this work, we consider two human body blockage models: multiple knife-edge diffraction [13, 9, 8] and elliptic cylinder [6] models, illustrated in Fig. 3. The elliptic cylinder model is an extension of the cylindrical human blockage model, described in [4] and aims at replicating the proportions of the human body. In our simulations, the elliptic cylinder is represented by a cylinder polygon with ten faces on the sides of the cylinder (the purpose of presenting cylinder as a polygon is to simplify meshing in the SBR software). Importantly, the human blockage models in our simulations have two-layer surface: the first layer is equivalent to the human skin and the second layer is assumed to resemble muscle tissues. The parameters for the human tissue are taken from [1] and are summarized in the Table 3.

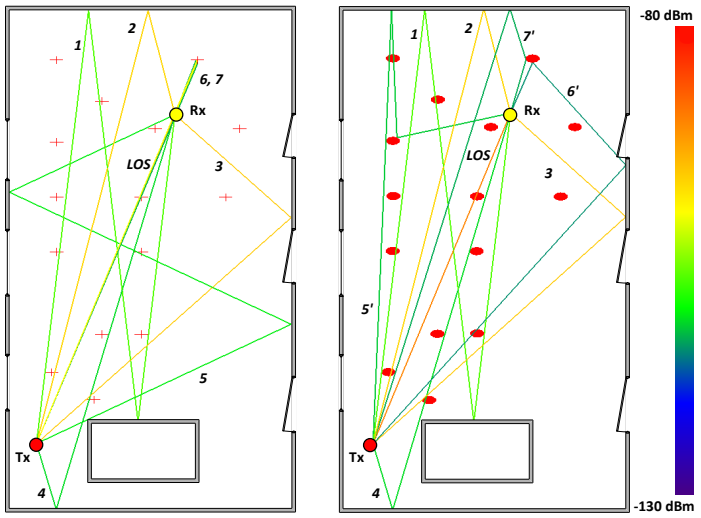

(a) MKED blockage model (b) Elliptic cylinder blockage model

Fig. 4: Paths of the most dominant rays at 60 GHz (Tx/Rx height is 2.5/1.6 m).

Here, the simulation is based on the same settings (including the environment and other parameters) as described in the previous section. The transmitter/receiver height is 2.5/1.6 m as the initial scenario advises. Fig. 4 demonstrates the difference between MKED and elliptic cylinder models in terms of propagation. While these models show similar results for the LOS path, there are some differences between MPCs of higher orders. Fig. 4 reveals that the LOS link exists for both models since the propagation path goes above all of the human blockers, which is due to the antenna heights. The rays from 1 to 4 are also retained since they are located far from the blockers (Fig. 4), and different blockage models do not affect these paths. However, as we may see, the rays from 5 to 7 are no longer present for the case, where the cylindrical model is used. If we examine ray №5 for the MKED case, we may observe that just before reaching the receiver, the ray passes very closely to the human body blockage model. Nevertheless, when the elliptic cylinder model is utilized, the ray №5 is blocked by one of the planes of the polygon cylinder (elliptic cylinder model) and cannot reach the receiver. Contrarily, the ray №5′ appears when the signal reflects from the wall after traveling above all of the potential blockers and reaching the receiver after the second reflection. Furthermore, we notice that rays 6 and 7, which rely upon the reflection from the blocker, also disappears. In case of elliptic cylinder model, we observe that these rays are replaced by rays №6′ and 7′ (although they are reflected from the walls of the room, which results in the loss of the received power).

As one may see, there is a difference between the propagating rays of higher orders in the MKED and elliptic cylinder models. However, it is also necessary to take into account such significant factors as the simulation time and computational resources. Fig. 5 shows the difference in the total simulation time that is required for equivalent experiments based on the models we study. For example, if we consider simulation with 5 people in the room the required time is 29 min for MKED model and 48 for the elliptic cylinder human blockage model. Further, if we consider 15 people in the room, the simulation time increases linearly for the MKED model and exponentially for the elliptic cylinder model, i.e., resulting in 55 min for MKED and 167 for the cylinder. Following computation times were measured on a computer with an Intel Core2Duo Q9500 CPU and Gigabyte nVidia GeForce GTX 550 Ti GPU with CUDA support. Given the total amount of the time required for modeling using elliptic cylinder model, we further focus only on the MKED human blockage model.

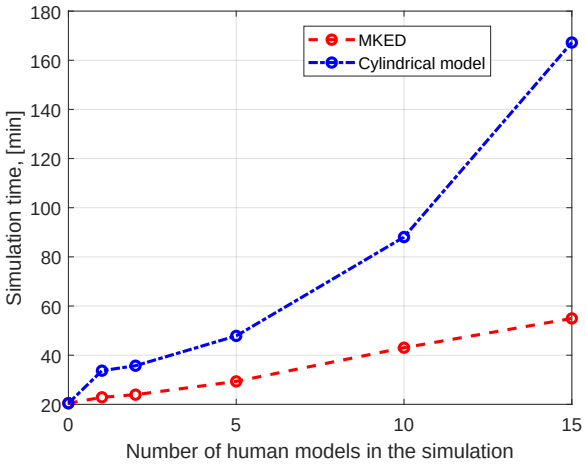

Fig. 5: Comparison of the simulation time for MKED and cylidrical models.

3.2 Channel characterization

Importantly, we demonstrate the results that correspond to the case, when there are 15 human blockers in the room. We intentionally omit the cases with less than 15 blockers as they produce mostly low-power components. For 15 human blockers scattered in the room, we observe a large number of first and second order MPCs with considerable powers (Fig. 6). These components mainly correspond to the rays reaching the receivers at the beginning of the trajectory. Apart from that, for certain locations the LOS link is no longer present since the receiver is right behind the blocker and signal is received only via the MPCs. Additional first and second order components appear because the rays are reflected from the blockers.

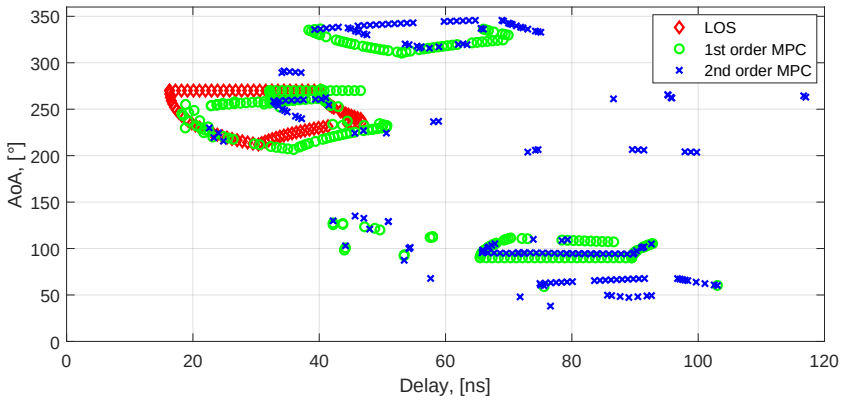

Fig. 6: Simulation results for LOS and dominant MPC at 60 GHz for the case of 15 people in the room.

Further, Fig. 7a shows a channel impulse response (CIR) at multiple receiver positions in the presence of 15 blockers as well as illustrates the dynamics of the delay when the receiver moves along the selected trajectory and blockage effects. For example, for the position №52 the LOS is blocked and only MPCs arrive at the receiver (Fig. 7b). In comparison, for the position №49 the LOS arrives at 46 ns. Since the distance difference between these positions is relatively small, the delay and power values for the LOS paths should be similar.

4 Simulation results for D2D scenario at 60 GHz

In this section, we consider a slightly different scenario, which represents interactions between wearable devices of different owners (e.g., as in a D2D scenario). The transmitter and receiver heights are set to 1.6 m, while the number of blockers remains 15 and the MKED model is used for modeling blockers. The receiver moves along the same trajectory of 100 positions as before, capturing the snapshots of the CIR. At the same time, the transmitter travels around the area in the conference room, where a small storeroom is located, and visits 18 positions (see Fig. 8). The snapshots of the CIR at the 60 GHz frequency are calculated for each of the transmitter/receiver positions. Based on the obtained results, we derive a logarithmic model [20] for the path loss:

$$L(d) = \alpha + 10\beta \log_{10}(d) + x, \tag{1}$$

where α and β are the parameters of the model and x is the random component, which reflects the effects of fading and is represented by a normally distributed variable with zero mean and standard deviation σ. Below we provide α, β, and σ for each of the components (Table 4). The path loss plots for the LOS case and first two orders MPCs are presented in Fig. 9.

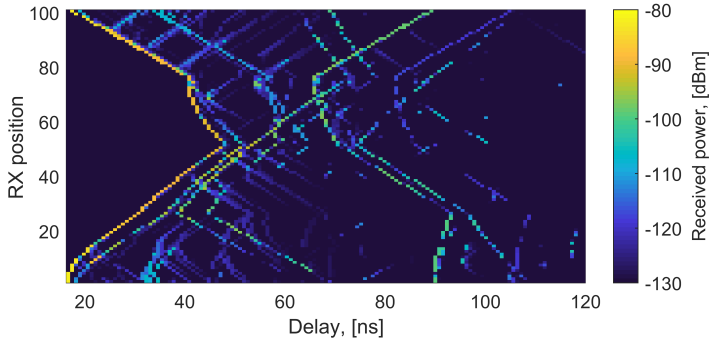

(a) CIR for all Rx positions

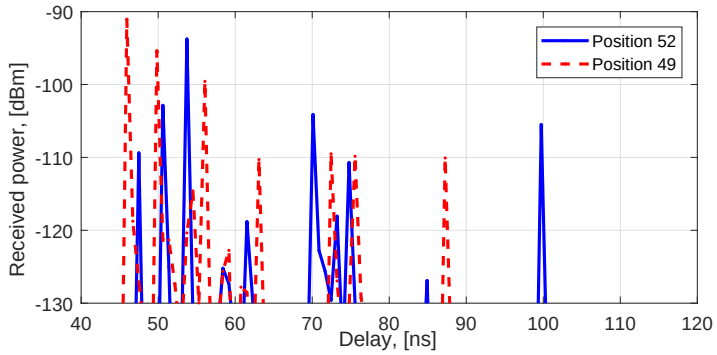

(b) CIR for the positions Nº49 and 52

Fig. 7: Channel impulse response at 60 GHz for the case of 15 people in the room.

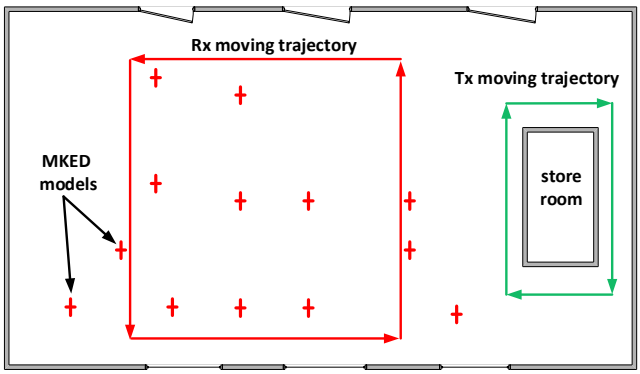

Fig. 8: A schematic view of the Rx and Tx positions in the conference room for the D2D scenario.

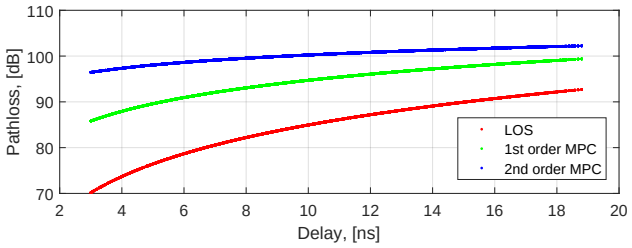

Fig. 9: Path loss model.

Table 4: Logarithmic model coefficients

Link type	α	β	σ
LOS	56.65	2.82	2.76
MPC-1	77.68	1.70	7.78
MPC-2	92.95	0.72	5.98

5 Conclusions and discussion

In this paper, we study the mmWave indoor propagation in the conference room scenario, for which the channel measurements at 83 GHz are openly available. In particular, having reconstructed a 3D model that is reasonably close to the environment of the measurement campaign, we calibrate our simulation with the available data. The difference is negligible and indicates that the reconstructed geometry of the room and the selected materials (that is, their electrical properties) are correctly adjusted.

Further, we study the radio wave propagation at 60 GHz, extending the said scenario by placing human blockers into the room. We compare two types of human blockage models and show that the MKED model is preferable in terms of simulation time, since the time increases exponentially for the elliptic cylinder model and almost linearly for the MKED model.

Finally, we consider a D2D scenario, which represents communications between, for example, hi-end wearable devices, and may support prospective augmented/virtual/hyper-reality applications. In particular, we analyze the angular delay profile for the LOS and MPCs at 60 GHz in the presence of blockers, as well as derive a corresponding logarithmic path loss model, which may be instrumental in the further evaluation of the MAC protocols performance and high-level system-level analysis.

Acknowledgment

The described research is supported in part by the National Sustainability Program under the grant LO1401. For the research, the infrastructure of the SIX Center was used. The work of Dr. Olga Galinina is supported by Finnish Cultural Foundation and personal Jorma Ollila grant.

References

1. Andreuccetti, D., Fossi, R., Petrucci, C.: An Internet Resource for the Calculation of the Dielectric Properties of Body Tissues in the Frequency Range 10 Hz - 100 GHz. Based on data published by C.Gabriel et al. in 1996. [Online]. Available: http://niremf.ifac.cnr.it/tissprop/ (1997)
2. Balanis, C.A.: Advanced engineering electromagnetics. John Wiley & Sons (1999)
3. Collonge, S., Zaharia, G., Zein, G.E.: Influence of the human activity on wide-band characteristics of the 60 GHz indoor radio channel. IEEE Transactions on Wireless Communications **3**(6), 2396–2406 (Nov 2004). https://doi.org/10.1109/TWC.2004.837276
4. Ghaddar, M., Talbi, L., Denidni, T.A., Sebak, A.: A Conducting Cylinder for Modeling Human Body Presence in Indoor Propagation Channel. IEEE Transactions on Antennas and Propagation **55**(11), 3099–3103 (Nov 2007). https://doi.org/10.1109/TAP.2007.908563
5. Ghaddar, M., Talbi, L., Denidni, T.A., Sebak, A.: A conducting cylinder for modeling human body presence in indoor propagation channel. IEEE Transactions on Antennas and Propagation **55**(11), 3099–3103 (2007)
6. Jacob, M.: The 60 GHz Indoor Radio Channel Overcoming the Challenges of Human Blockage. Ph.D. thesis, Technische Universität Braunschweig (2013)
7. Jacob, M., Mbianke, C., Krner, T.: A dynamic 60 ghz radio channel model for system level simulations with mac protocols for ieee 802.11ad. In: IEEE International Symposium on Consumer Electronics (ISCE 2010). pp. 1–5 (June 2010). https://doi.org/10.1109/ISCE.2010.5523241
8. Jacob, M., Priebe, S., Kürner, T., Peter, M., Wisotzki, M., Felbecker, R., Keusgen, W.: Fundamental analyses of 60 GHz human blockage. In: The 7th European Conference on Antennas and Propagation (EuCAP). pp. 117–121 (April 2013)
9. Jacob, M., Priebe, S., Maltsev, A., Lomayev, A., Erceg, V., Kürner, T.: A ray tracing based stochastic human blockage model for the IEEE 802.11ad 60 GHz channel model. In: The 5th European Conf. on Ant. and Prop. (EuCAP2011). pp. 3084–3088. Rome, Italy (April 2011)
10. Jacob, M., Priebe, S., Maltsev, A., Lomayev, A., Erceg, V., Krner, T.: A ray tracing based stochastic human blockage model for the ieee 802.11ad 60 ghz channel model. In: Proceedings of the 5th European Conference on Antennas and Propagation (EUCAP). pp. 3084–3088 (April 2011)
11. Khafaji, A., Saadane, R., El Abbadi, J., Belkasmi, M.: Ray tracing technique based 60 GHz band propagation modelling and influence of people shadowing. International Journal of Electrical, Computer, and Systems Engineering **2**(2), 102–108 (2008)
12. Kovalchukov, R., Samuylov, A., Moltchanov, D., Ometov, A., Andreev, S., Koucheryavy, Y., Samouylov, K.: Modeling three-dimensional interference and sir in highly directional mmwave communications. In: Proc. of IEEE Global Communications Conference. pp. 1–7. IEEE (2017)
13. Kunisch, J., Pamp, J.: Ultra-wideband double vertical knife-edge model for obstruction of a ray by a person. In: 2008 IEEE International Conference on Ultra-Wideband. vol. 2, pp. 17–20 (Sept 2008). https://doi.org/10.1109/ICUWB.2008.4653341
14. Kunisch, J., Pamp, J.: Ultra-wideband double vertical knife-edge model for obstruction of a ray by a person. In: Ultra-Wideband, 2008. ICUWB 2008. IEEE International Conference on. vol. 2, pp. 17–20. IEEE (2008)

15. Lai, D., Wang, J., Gentile, C., Papazian, P., Choi, J.K., Senic, J., Golmie, N., Remley, K.: Multipath Component Tracking and Channel Model for Lecture Room. Standard, Document IEEE 802.11-16/846-ay (July 2016), https://mentor.ieee.org/802.11/dcn/16/11-16-0846-00-00ay-multipath-component-tracking-and-channel-model-for-lecture-room.pptx
16. Maltsev, A.: Channel models for 60GHz WLAN systems. IEEE802. 11 09/0334r8 (2010)
17. METIS, M.: Wireless communications Enablers for the Twenty-twenty Information Society, EU 7th Framework Programme project. Tech. rep., ICT-317669-METIS
18. Pathak, P., Burnside, W., Marhefka, R.: A uniform GTD analysis of the diffraction of electromagnetic waves by a smooth convex surface. IEEE Transactions on antennas and propagation **28**(5), 631–642 (1980)
19. Peter, M., Wisotzki, M., Raceala-Motoc, M., Keusgen, W., Felbecker, R., Jacob, M., Priebe, S., Krner, T.: Analyzing human body shadowing at 60 ghz: Systematic wideband mimo measurements and modeling approaches. In: 2012 6th European Conference on Antennas and Propagation (EUCAP). pp. 468–472 (March 2012). https://doi.org/10.1109/EuCAP.2012.6206013
20. Rappaport, T.S., et al.: Wireless communications: principles and practice, vol. 2. prentice hall PTR New Jersey (1996)
21. Smulders, P.F.: Statistical characterization of 60-GHz indoor radio channels. IEEE Transactions on Antennas and Propagation **57**(10), 2820–2829 (2009)
22. Solomitckii, D., Semkin, V., Naderpour, R., Ometov, A., Andreev, S.: Comparative evaluation of radio propagation properties at 15 ghz and 60 ghz frequencies. In: Proc. of 9th International Congress on Ultra Modern Telecommunications and Control Systems and Workshops (ICUMT). pp. 91–95. IEEE (2017)
23. Sum, C.S., Lan, Z., Funada, R., Wang, J., Baykas, T., Rahman, M., Harada, H.: Virtual time-slot allocation scheme for throughput enhancement in a millimeter-wave multi-Gbps WPAN system. IEEE Journal on Selected Areas in Communications **27**(8) (2009)
24. Tai, C.T.: Dyadic Green functions in electromagnetic theory. Institute of Electrical & Electronics Engineers (IEEE) (1994)
25. Tang, C.C.: Backscattering from Dielectric-Coated Infinite Cylindrical Obstacles. Journal of Applied Physics **28**(5), 628–633 (1957)
26. Venugopal, K., Valenti, M.C., Heath, R.W.: Device-to-device millimeter wave communications: Interference, coverage, rate, and finite topologies. IEEE Transactions on Wireless Communications **15**(9), 6175–6188 (2016)
27. Zhu, X., Doufexi, A., Kocak, T.: Throughput and coverage performance for ieee 802.11ad millimeter-wave wpans. In: 2011 IEEE 73rd Vehicular Technology Conference (VTC Spring). pp. 1–5 (May 2011). https://doi.org/10.1109/VETECS.2011.5956194